IEEE Access
Multidisciplinary | Rapid Review | Open Access Journal

Received October 26, 2018, accepted November 6, 2018, date of publication November 12, 2018,
date of current version December 19, 2018.

Digital Object Identifier 10.1109/ACCESS.2018.2880885

Research on the Acoustic-Structure Coupling Characteristics of a Piezoelectric Micro-Jet Used for Lubricating

KAI LI[1], JUNKAO LIU[1], HENGYU LI[1], NAIMING QI[2], AND WEISHAN CHEN[1]
[1]State Key Laboratory of Robotics and System, Harbin Institute of Technology, Harbin 150001, China
[2]School of Astronautics, Harbin Institute of Technology, Harbin 150001, China

Corresponding author: Weishan Chen (cws@hit.edu.cn)

This work was supported in part by the National Natural Science Foundation of China under Grant 51475112 and Grant 51622502 and in part by the Foundation for Innovative Research Groups of the National Natural Science Foundation of China under Grant 51521003.

ABSTRACT The injection performance of the piezoelectric micro-jet is mainly determined by the acoustic characteristics created in the cavity by the vibration of the piezoelectric vibrator. As sensors are difficult to be placed into the cavity of the piezoelectric micro-jet, the inside acoustic characteristics are hard to be tested by experiments. Thus, an acoustic-structure coupling model is given, and simulation analyses are carried out in this paper to study a piezoelectric micro-jet used for lubricating. The suitable working frequency for getting better lubricating performance is obtained by the frequency response characteristics analyses. The driving mechanism is revealed by comparing with the injection results. The influences of excitations on the acoustic pressure at the nozzle part are analyzed, and the methods for adjusting the working performance are obtained. The acoustic structure coupling model and results are verified by comparing with the experiment results.

INDEX TERMS Acoustic-structure coupling, lubricating, micro injection, piezoelectric devices.

I. INTRODUCTION

Piezoelectric actuators have been widely used in fields requiring precise actuation due to their high precision and quick response [1]–[3]. The piezoelectric micro-jet is a kind of device which is based on piezoelectric actuation and can achieve the requirement of drop on demand. Nowadays, it is wildly applied to many industrial fields, such as rapid prototyping [4]–[8], medical treatment [9], [10], biology [11], [12], sensors [13], [14], etc. The working stages of the piezoelectric micro-jet can be divided into driving stage and ejecting stage. The acoustic pressure waves are created and propagate during driving stage which mainly involves acoustic structure coupling. The droplets are formed and ejected out during injection stage, which mainly involves two phase flow coupling. In order to obtain the influences of structure sizes and bubbles on the injection performance, the acoustic structure coupling characteristics of piezoelectric micro-jet are mainly studied by experiments, simulations or self-sensing measurements [15]–[20]. The two phase flow coupling characteristics are mainly analyzed based on experiments and fluid dynamics simulations, by which the effects of excitation on the droplet forming process can be obtained [21]–[24]. The injection performance of piezoelectric micro-jet depends on the driving characteristics inside the cavity. By analyzing the acoustic characteristics in the cavity, the driving mechanism can be revealed and the method to control the injection performance during the driving stage can be obtained.

In general, the shell of the piezoelectric is non transparent and the sensor is not easy to be placed in the cavity. Thus, it is limited to study the acoustic structure coupling characteristics inside the cavity by experiments. For using the method of self-sensing measurement, complex decoupling calculations are required. Therefore, simulations are usually simple, effective and most commonly used research method. At present, analyses generally focused on the nozzle part [25]–[28], but the bidirectional coupling effects between piezoelectric vibrator and fluid is often neglected, which can reduce the accuracy of calculation. Thus, for analyzing the driving state of piezoelectric micro-jet, bidirectional acoustic structure coupling analyses should be carried out.

In our previous work, a piezoelectric micro-jet used for bearing lubricating was designed, the influences of excitations on the formation and motion of ejected droplets are were analyzed, and the method for controlling the performance of

ejecting stage were given [14]. In order to reveal the driving mechanism of the designed piezoelectric micro-jet and obtain the method for controlling the injection performance during the driving stage, the acoustic structure coupling characteristics of the piezoelectric micro-jet are analyzed in this work. As the cavity is filled with lubricating oil and the shell is made of non-transparent metal material, an acoustic structure coupling model, which is universal for general piezoelectric micro-jet, is given. The frequency response characteristics of the piezoelectric micro-jet are analyzed based on this model, and the frequency of excitation pulse for getting better working performance is obtained. The influences of amplitude and duty ratio of pulse voltage on the nozzle pressure are analyzed, and the method to control the injection performance during the driving stage is given. By comparing the obtained coupling results with the dynamics results of droplet which are obtained in our previous work, the driving mechanism of the piezoelectric micro-jet is revealed. Experiments are carried out to verify the feasibility of the coupling model.

II. ACOUSTIC STRUCTURE MODEL

The working principle of the piezoelectric micro-jet is described as shown in Fig.1. When pulse voltages are applied on the piezoelectric vibrator, the piezoelectric vibrator vibrates and the acoustic pressure waves are created in the cavity. The created pressure waves propagate through the fluid in the cavity and can be reflected at the inside wall surface of the cavity. Then the droplet is ejected by the superposition pressure waves propagating to the nozzle.

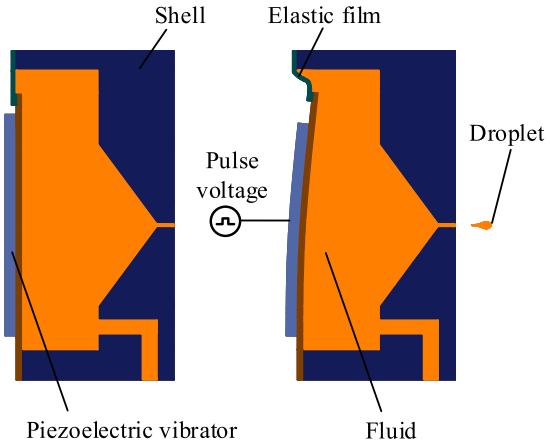

FIGURE 1. The working principle of the piezoelectric micro-jet.

A. BOUNDARY CONDITION

The acoustic pressure waves, which are created by the vibrations of piezoelectric vibrator, propagate through the fluid in the cavity. When pressure waves propagate to the wall of the cavity, the reflection and refraction of the waves are created. When pressure waves propagate in a two-dimensional plane, the reflection and refraction state of the waves can be described as shown in Fig.2, where the left field of the solid line is the inner side of the cavity, the right field is the wall of the cavity, and the dotted line is the normal direction of the interface. θ_i, θ_r and θ_t are the incident angle, reflection angle and refraction angle, respectively.

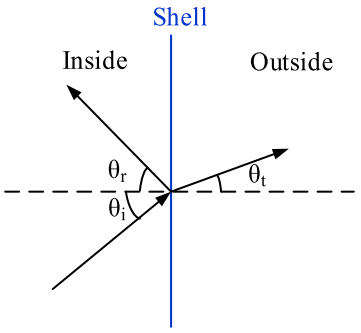

FIGURE 2. The reflection and refraction state of acoustic wave at the interface.

The incident acoustic pressure wave can be expressed as:

$$p_i(t,x,y) = p_{ia}e^{j(wt-kx\cos\theta_i-ky\sin\theta_i)}$$
$$w = 2\pi f, \quad k = \frac{2\pi f}{c_0} \tag{1}$$

where x, y are the coordinate values in the two-dimensional plane, p_i is the acoustic pressure of the incident acoustic wave, f is the frequency of the acoustic wave, c_0 is the sound velocity of the acoustic wave inside the cavity, p_{ia} is the acoustic pressure amplitude of the incident acoustic wave.

The reflection acoustic pressure wave can be expressed as:

$$p_r(t,x,y) = p_{ra}e^{j(wt+kx\cos\theta_r-ky\sin\theta_r)} \tag{2}$$

where p_r is the acoustic pressure of the reflection acoustic wave, p_{ra} is the acoustic pressure amplitude of the reflection acoustic wave.

Thus, the acoustic wave inside the cavity is the superposition of the incident and reflected waves:

$$\begin{aligned} p_{in} &= p_i + p_r \\ &= p_{ia}e^{j(wt-kx\cos\theta_i-ky\sin\theta_i)} + p_{ra}e^{j(wt+kx\cos\theta_r-ky\sin\theta_r)} \end{aligned} \tag{3}$$

where p_{in} is the acoustic pressure inside the cavity.

The refraction acoustic pressure wave can be expressed as:

$$p_t(t,x,y) = p_{ta}e^{j(wt-k'x\cos\theta_r-k'y\sin\theta_r)}$$
$$w = 2\pi f, \quad k' = \frac{2\pi f}{c_0'} \tag{4}$$

where p_t is the acoustic pressure of the refraction acoustic wave, p_{ta} is the acoustic pressure amplitude of the refraction acoustic wave, c_0' is the sound velocity of the acoustic wave into the shell.

Acoustic pressure balance should be satisfied at the interface:

$$p_{in} = p_i + p_r = p_t \tag{5}$$

Thus, the equation of acoustic pressure balance at the interface can be described as:

$$p_{ia}e^{j(wt-ky\sin\theta_i)} + p_{ra}e^{j(wt-ky\sin\theta_r)} = p_{ta}e^{j(wt-k'y\sin\theta_r)} \tag{6}$$

Based on the momentum conservation equation, the equation of the normal acceleration of fluid at the interface can be described as:

$$\frac{\partial v_n}{\partial t} = \{n\} \cdot \frac{\partial \{v\}}{\partial t} = -(\frac{1}{\rho_0} + \frac{4\eta}{3\rho_0^2 c_0^2}\frac{\partial}{\partial t})\{n\} \cdot \nabla p \quad (7)$$

where, v_n is the normal velocity of fluid at the interface, $\{v\}$ is the velocity vector of fluid, $\{n\}$ is the normal unit vector, η is the hydrodynamic viscosity coefficient of the ejected fluid, ρ_0 is the density of the fluid, c_0 is the sound velocity of the acoustic wave in fluid.

B. COUPLING MODEL

For piezoelectric micro-jet ejecting viscous fluid, the acoustic wave equation can be described as [29]:

$$\nabla \cdot (\frac{1}{\rho_0}\nabla p_i) - \frac{1}{\rho_0 c_0^2}\frac{\partial^2 p_i}{\partial t^2} + \nabla \cdot [\frac{4\eta}{3\rho_0}\nabla(\frac{1}{\rho_0 c_0^2}\frac{\partial p_i}{\partial t})] = 0 \quad (8)$$

By combining the acoustic wave equation with the boundary condition equations, the acoustic finite element simulation model is obtained:

$$[M_f]\{\ddot{P}\} + [C_f]\{\dot{P}\} + [K_f]\{P\} + \rho_0[R]\{\ddot{U}_f\} = \{F_f\} \quad (9)$$

where, $\{U_f\}$, $\{F_f\}$ are fluid displacement vectors and load vectors of fluid respectively, $[M_f]$, $[C_f]$ are fluid mass matrix and damping matrix respectively, $[K_f]$, $[R]$ are fluid stiffness matrix and boundary matrix respectively, $\{P\}$ is the fluid pressure vector.

Combining with the equation of motion, the acoustic structure model for simulation can be described as:

$$\begin{bmatrix} [M_s] & 0 \\ \rho[R] & [M_f] \end{bmatrix}\begin{Bmatrix} \ddot{U} \\ \ddot{P} \end{Bmatrix} + \begin{bmatrix} [C_s] & 0 \\ 0 & [C_f] \end{bmatrix}\begin{Bmatrix} \dot{U} \\ \dot{P} \end{Bmatrix} + \begin{bmatrix} [K_f] & -[R] \\ 0 & [K_f] \end{bmatrix}\begin{Bmatrix} U \\ P \end{Bmatrix} = \begin{Bmatrix} F_s \\ F_f \end{Bmatrix} \quad (10)$$

where $[M_s]$, $[K_s]$ are the mass matrix and stiffness matrix of the diaphragm respectively, $\{U\}$ is the displacement vector of the fluid/diaphragm at the coupling surface, $\{F_s\}$ is the vector sum of driving force and fluid reaction force of piezoelectric ceramic, $[C_s]$ is the damping matrix of the diaphragm.

In this work, the pressure balances and acceleration at the boundary are obtained based on Eq.(6) and Eq.(7), the acoustic characteristics inside the cavity are studied based on Eq.(9), the acoustic structure coupling between the vibrator and fluid is studied based on Eq.(10). It can be seen from Fig.1 that the incident and reflection acoustic waves propagate inside the cavity. In order to improve the utilization rate of vibration energy, large magnitude of the reflection wave is required. From Eq.(6), it can be seen that the magnitude of reflection wave is closely related to its amplitude and the phase difference between incident wave and refraction wave. The phase difference is depended on the material of the cavity, thus, when the cavity strength meets the requirements, the material that can achieve total reflection should be chosen based on Eq.(6). As the amplitude of the reflection wave is mainly related to the excitation signal, the influences of the excitation parameters on the working performance of the piezoelectric micro-jet are analyzed in this work. Due to the difficulties to obtain the analytical solution, the finite element analysis software ANSYS (ANSYS, Inc) is used in this work to carry on the numerical simulations.

III. FREQUENCY RESPONSE CHARACTERISTIC ANALYSIS

In our previous work, the formation and motion statuses of the droplet are mainly studied, but how to determine the working frequency of the piezoelectric micro-jet used for lubricating is not done. The schematic diagram and finite element model of the piezoelectric micro-jet used for lubricating are shown in Fig.3 and Fig.4, respectively, where blue arrows represent the oil supply path. The piezoelectric vibrator is made by gluing the piezoelectric ceramic onto the copper film. The inner ring of the vibrator is fixed and the outer ring is connected with the sealed elastic film. When pulse voltages are applied on the piezoelectric vibrator, the oil droplets are ejected out of the nozzle and move to the target bearings.

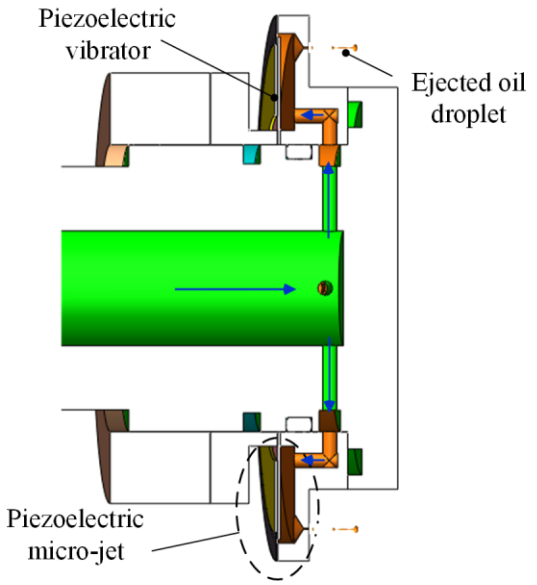

FIGURE 3. The schematic diagram of the piezoelectric micro-jet.

FLUID30 is selected as the element type of the oil. The piezoelectric ceramic and the copper film are modeled with SOLID226 and SOLID185 respectively. The acoustic impedance of the outer surface of the liquid is set as $17.1\times10^6 \mathrm{kg{\cdot}m^{-2}\cdot s^{-1}}$ which depend on the outermost shell (whose material is aluminum) of the micro-jet. The acoustic impedance at the nozzle is set as 400 $\mathrm{kg{\cdot}m^{-2}\cdot s^{-1}}$ which depend on the properties of the air. The acoustic impedances of the material can be obtained through relevant reference [30]. The density, elasticity modulus and Poisson ratio of the copper film are 7.5×10^3 $\mathrm{kg/m^3}$, 7.65×10^{10} $\mathrm{N/m^2}$ and 0.32, respectively. The material of the piezoelectric ceramic is PZT-5H, and its physical properties (elastic stiffness constant matrix $[c^E]$, piezoelectric stress constant matrix $[e]$ and

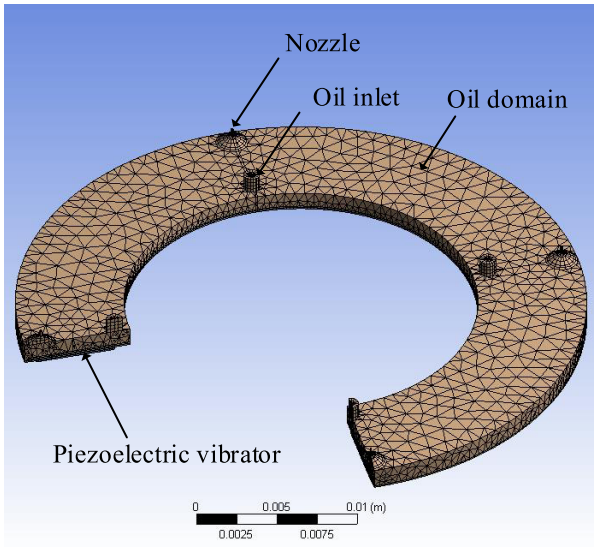

FIGURE 4. The finite element model (three fourths) of the piezoelectric micro-jet for acoustic structure coupling simulations.

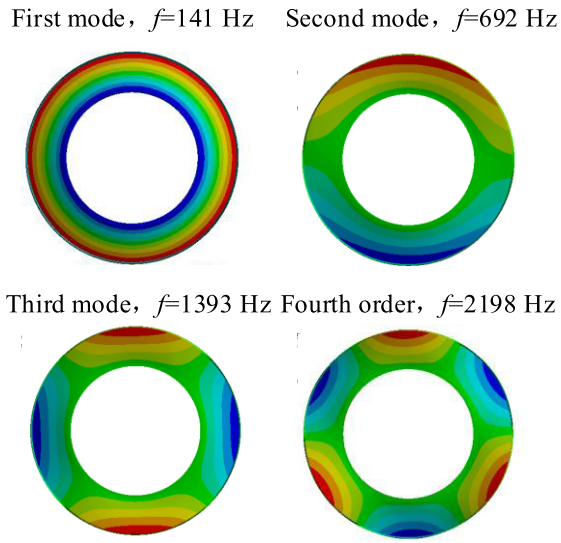

FIGURE 5. The modes of vibrator with coupling effect.

dielectric constant matrix $[\varepsilon^{\mathrm{T}}]$) are set as:

$$[c^{\mathrm{E}}] = \begin{bmatrix} 13.2 & 7.3 & 7.1 & 0 & 0 & 0 \\ 7.3 & 13.2 & 7.1 & 0 & 0 & 0 \\ 7.1 & 7.1 & 11.5 & 0 & 0 & 0 \\ 0 & 0 & 0 & 2.6 & 0 & 0 \\ 0 & 0 & 0 & 0 & 2.6 & 0 \\ 0 & 0 & 0 & 0 & 0 & 3 \end{bmatrix} \times 10^{10}(\mathrm{N/m^2}) \quad (11)$$

$$[e] = \begin{bmatrix} 0 & 0 & -2.4 \\ 0 & 0 & -2.4 \\ 0 & 0 & 17.3 \\ 0 & 0 & 0 \\ 0 & 12.95 & 0 \\ 12.95 & 0 & 0 \end{bmatrix} (\mathrm{C/m^2}) \quad (12)$$

$$[\varepsilon^{\mathrm{T}}] = \begin{bmatrix} 804.6 & 0 & 0 \\ 0 & 804.6 & 0 \\ 0 & 0 & 659.7 \end{bmatrix} \times 10^{-11}(\mathrm{F/m}) \quad (13)$$

Based on the acoustic structure coupling analysis, the working frequency can be obtained. When the cavity of the piezoelectric micro-jet is filled with lubricating oil, the first four order modes is shown in Fig.5, and the frequency response characteristic curve of pressure at the nozzle is shown in Fig.5.

As shown in Fig.3, four nozzles are designed on the piezoelectric micro-jet for uniform lubrication. Based on the results shown in Fig.5, oil droplet can be ejected from four nozzles when the vibrator works in the first mode. When the vibrator works in other modes, the vibration shapes are asymmetrical which will cause the fluid in the cavity to move in a circumferential direction and energy loss is created. As we can see form Fig.6, the frequency corresponding to the peak point of the curve is the frequency of the first mode, and the nozzle pressures when the vibrator works in other modes

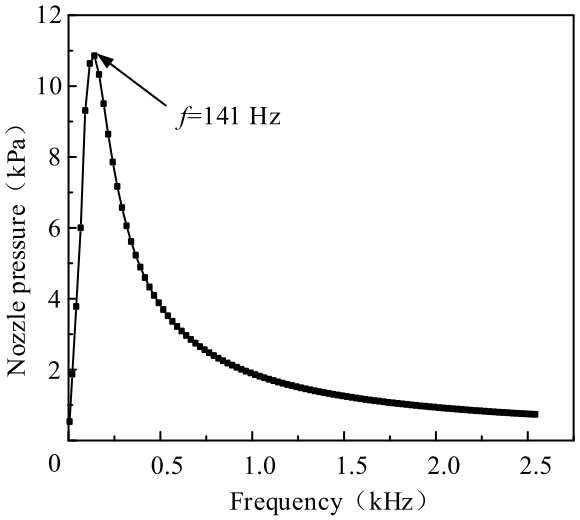

FIGURE 6. The frequency response of nozzle pressure.

are relatively low. Thus, the first mode with the frequency of 141 Hz should be selected as the working mode of the vibrator.

IV. TRANSIENT ANALYSIS

When pulse square waves with amplitude as 200V and duty ratio as 0.5 are applied on the piezoelectric vibrator, the change curves of the nozzle pressure various with different frequencies in one period are shown in Fig.7, where T is expressed as the pulse period. It can be seen that when excitation with relative low frequency is applied, the pressure wave propagating to the nozzle presents fluctuation state which will cause the energy loss of acoustic pressure wave. With the increase of the frequency value, the pressure fluctuation gradually decreases and tends to be smooth. It also can be seen that, the absolute value of the peak of negative

pressure at the nozzle increases first and then decreases, and the maximum value occurs when the frequency is 140 Hz (first mode). Comparing with the results of [14], we can see that the absolute value of the peak of negative pressure affects the reflux strength of oil when the droplet is detached from the nozzle. The greater the reflux intensity is, the easier the droplet is ejected from the nozzle.

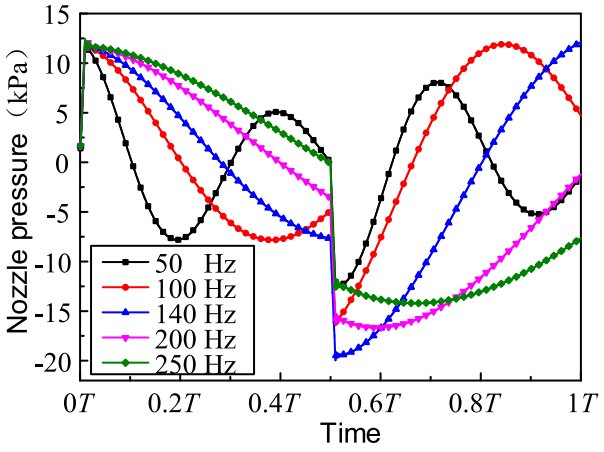

FIGURE 7. The nozzle pressure under excitation with different frequencies.

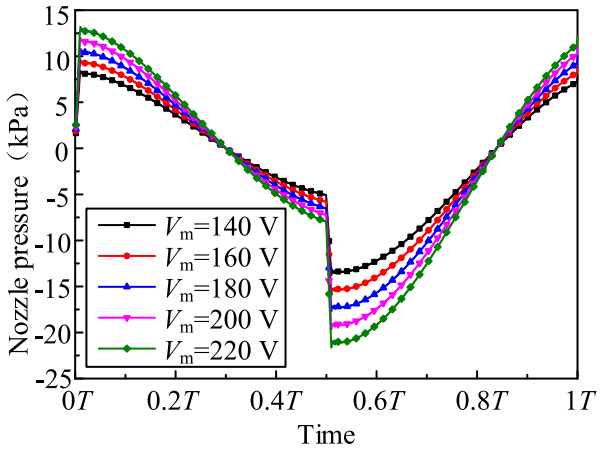

FIGURE 8. The nozzle pressure under excitation with different amplitude.

Based on the results from Fig.5, Fig.6 and Fig.7, the working frequency of the piezoelectric vibrator should be 141 Hz. When pulse square waves with duty ratio as 0.5 and frequency as 141 Hz are applied on the piezoelectric vibrator, the change curves of the nozzle pressure various with different wave amplitudes are shown in Fig.8, where V_m represents the amplitude of the pulse voltage. It can be seen that, the sudden changes of nozzle pressure occur in the stages of switching pulse voltage levels (switch low/high level to high/low level). The reason is that, when the pulse voltages level switches, the piezoelectric vibrator creates rapid deformation, which results in the rapid change of the nozzle pressure. We can also see that, the amplitude of the pulse voltage influences little on the change trend of the nozzle pressure, while the peak value of the nozzle pressure increases along with the increase of the wave amplitude. Thus, the injection intensity of the piezoelectric micro-jet can be controlled by adjusting the amplitude of the pulse voltage.

When pulse square waves with amplitude as 200V and frequency as 141 Hz are applied on the piezoelectric vibrator, the change curves of the nozzle pressure various with different wave duty ratios are shown in Fig.9, where α represents the duty ratio.

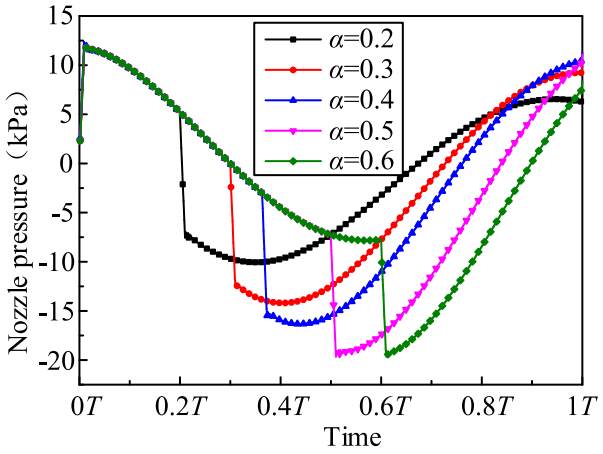

FIGURE 9. The nozzle pressure under excitation with different duty ratios.

It can be seen that the influences of the duty ratio on the nozzle pressure is mainly created after the level of the pulse voltage changing from high to low. With the increase of the duty ratio, the time taken for the nozzle pressure to reach the peak of the negative pressure increases, which is consistent with the time when the level of the excitation changes from high to low. Comparing with the results of [15], we can see that due to the suddenly occurred negative pressure at the nozzle which is resulted by the excitation level changing, reflux of the oil, which is connected with the forming droplet and inside the cavity, is created. While, under the action of the inertial force, the formed droplet continue moves outside the nozzle. Then, the reflux effect and the inertial force make the droplet be ejected out of the nozzle. Besides, the absolute value of the peak of negative pressure increases along with the increase of duty ratio, which means that when the injection intensity meets the requirements, the response rate can be increased by reducing the duty ratio.

V. EXPERIMENTS

As it is difficult to test the acoustic characteristics inside the cavity which is filled with lubricating oil, here we only verify the influences of amplitude of the pulse voltage on the injection performance. The experimental setup details can be found in [14].

When excitations with duty ratio as 0.5 and frequency as 141Hz are applied on the piezoelectric vibrator, the injection

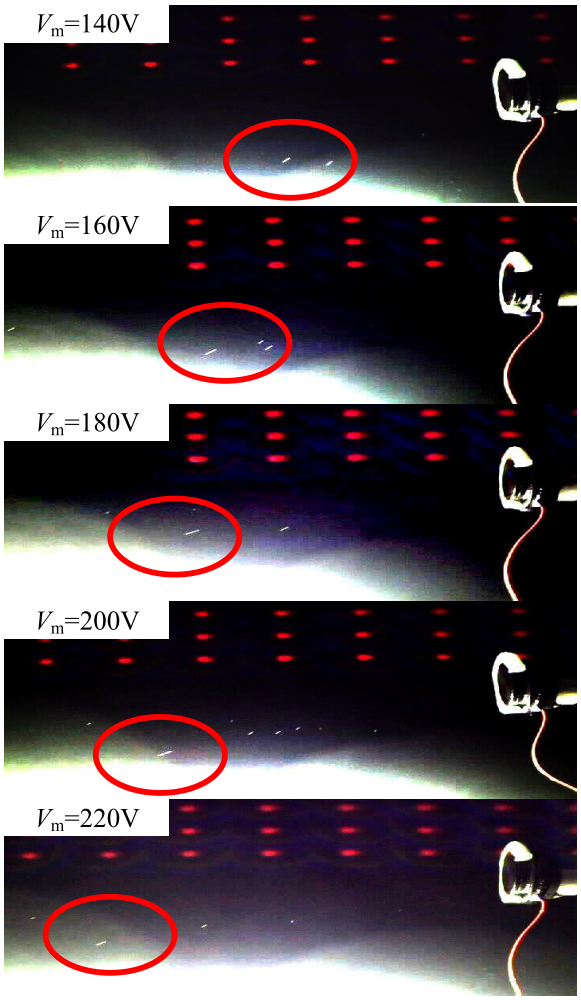

FIGURE 10. The injection statuses under excitation with different voltage amplitudes.

statuses of the piezoelectric micro-jet various with different wave amplitude are shown in Fig.10.

It can be seen that with the increase of the amplitude the injection intensity increase gradually. Comparing the test results with the acoustic structure results, the acoustic structure model and simulation results are verified to be effective.

VI. CONCLUSIONS

In order to study the acoustic structure coupling characteristics of general piezoelectric micro-jet, the acoustic structure model is given. Based on the developed model, a piezoelectric micro-jet used for lubricating is studied, and the working frequency for obtained better performance is given. The influences of the excitation parameters are analyzed, and the methods to control the working performance in the driving stage are given. By comparing with the results of previous work, the driving mechanism is obtained: the droplet is ejected out by the joint action of the inertial force and the reflux of fluid; the inertial force is created by the excitation when excitation changing to high level; the reflux of the fluid is created due to the suddenly occurred negative pressure created when excitation changing to low level. The acoustic structure model and results are verified by experiments.

REFERENCES

[1] S. He, P. R. Chiarot, and S. Park, "A single vibration mode tubular piezoelectric ultrasonic motor," *IEEE Trans. Ultrason., Ferroelectr., Freq. Control*, vol. 58, no. 5, pp. 1049–1061, May 2011.

[2] G. Y. Gu, L. M. Zhu, C. Y. Su, H. Ding, and S. Fatikow, "Proxy-based sliding-mode tracking control of piezoelectric-actuated nanopositioning stages," *IEEE/ASME Trans. Mechatronics*, vol. 20, no. 4, pp. 1956–1965, Aug. 2015.

[3] Y. Liu, W. Chen, J. Liu, and X. Yang, "A high-power linear ultrasonic motor using bending vibration transducer," *IEEE Trans. Ind. Electron.*, vol. 60, no. 11, pp. 5160–5166, Nov. 2013.

[4] C.-L. Lee, K.-C. Chang, and C.-M. Syu, "Silver nanoplates as inkjet ink particles for metallization at a low baking temperature of 100 °C," *Colloids Surfaces A, Physicochem. Eng. Aspects*, vol. 381, pp. 85–91, May 2011.

[5] I. Salaoru, Z. Zhou, P. Morris, and G. J. Gibbons, "Inkjet printing of polyvinyl alcohol multilayers for additive manufacturing applications," *J. Appl. Polymer Sci.*, vol. 133, no. 25, Jul. 2016, Art. no. 43572.

[6] B. Andò, S. Baglio, A. R. Bulsara, V. Marletta, V. Ferrari, and M. Ferrari, "A low-cost snap-through-buckling inkjet-printed device for vibrational energy harvesting," *IEEE Sensors J.*, vol. 15, no. 6, pp. 3209–3220, Jun. 2015.

[7] V. H. Schmidt, L. Lediaev, J. Polasik, and J. Hallenberg, "Piezoelectric actuators employing PVDF coated with flexible PEDOT-PSS polymer electrodes," *IEEE Trans. Dielectr. Electr. Insul.*, vol. 13, no. 5, pp. 1140–1148, Oct. 2006.

[8] T. M. Lee *et al.*, "Drop-on-demand solder droplet jetting system for fabricating microstructure," *IEEE Trans. Electron. Packag. Manuf.*, vol. 31, no. 3, pp. 202–210, Jul. 2008.

[9] R. D. Boehm, P. R. Miller, W. A. Schell, J. R. Perfect, and R. J. Narayan, "Inkjet printing of amphotericin B onto biodegradable microneedles using piezoelectric inkjet printing," *J. Minerals, Met. Mater. Soc.*, vol. 65, pp. 525–533, Apr. 2013.

[10] R. Haj-Ahmad *et al.*, "Microneedle coating techniques for transdermal drug delivery," *Pharmaceutics*, vol. 7, pp. 486–502, Dec. 2015.

[11] Y. Sun, X. Zhou, and Y. Yu, "A novel picoliter droplet array for parallel real-time polymerase chain reaction based on double-inkjet printing," *Lab Chip*, vol. 14, no. 18, pp. 3603–3610, 2014.

[12] C. Tse *et al.*, "Inkjet printing Schwann cells and neuronal analogue NG108-15 cells," *Biofabrication*, vol. 8, no. 1, p. 015017, Mar. 2016.

[13] C. J. Sielmann, J. R. Busch, B. Stoeber, and K. Walus, "Inkjet printed all-polymer flexural plate wave sensors," *IEEE Sensors J.*, vol. 13, no. 10, pp. 4005–4013, Oct. 2013.

[14] K. Li, J. Liu, R. Yang, W. Chen, L. Zhang, and Y. Liu, "A trace redundant lubrication piezoelectric microjet for bearing system," *IEEE/ASME Trans. Mechatronics*, vol. 23, no. 5, pp. 2263–2272, Oct. 2018.

[15] H.-C. Wu and H.-J. Lin, "Effects of actuating pressure waveforms on the droplet behavior in a piezoelectric inkjet," *Mater. Trans.*, vol. 51, pp. 2269–2276, Dec. 2010.

[16] S. Kim, J. Sung, and M. H. Lee, "Pressure wave and fluid velocity in a bend-mode inkjet nozzle with double PZT actuators," *J. Thermal Sci.*, vol. 22, pp. 29–35, Feb. 2013.

[17] H.-J. Lin, H.-C. Wu, T.-R. Shan, and W.-S. Hwang, "The effects of operating parameters on micro-droplet formation in a piezoelectric inkjet printhead using a double pulse voltage pattern," *Mater. Trans.*, vol. 47, pp. 375–382, Feb. 2006.

[18] B.-H. Kim *et al.*, "A study of the jetting failure for self-detected piezoelectric inkjet printheads," *IEEE Sensors J.*, vol. 11, no. 12, pp. 3451–3456, Dec. 2011.

[19] A. van der Bos *et al.*, "Infrared imaging and acoustic sizing of a bubble inside a micro-electro-mechanical system piezo ink channel," *J. Appl. Phys.*, vol. 110, p. 034503, Aug. 2011.

[20] B. H. Kim *et al.*, "A study of the jetting failure for self-detected piezoelectric inkjet printheads," *IEEE Sensors J.*, vol. 11, no. 12, pp. 3451–3456, Dec. 2011.

[21] M. H. Tsai, W. S. Hwang, and H. H. Chou, "The micro-droplet behavior of a molten lead-free solder in an inkjet printing process," *J. Micromech. Microeng.*, vol. 19, no. 12, p. 125021, Dec. 2009.

[22] S. Desai and M. Lovell, "Modeling fluid–structure interaction in a direct write manufacturing process," *J. Mater. Process. Technol.*, vol. 212, pp. 2031–2040, Oct. 2012.
[23] J. Chang, Y. Liu, and B. Huang, "Steady state response analysis of a tubular piezoelectric print head," *Sensors*, vol. 16, no. 1, p. 81, Jan. 2016.
[24] K.-S. Kwon, "Waveform design methods for piezo inkjet dispensers based on measured meniscus motion," *J. Microelectromech. Syst.*, vol. 18, no. 5, pp. 1118–1125, Oct. 2009.
[25] T.-M. Liou, C.-Y. Chan, and K.-C. Shih, "Effects of actuating waveform, ink property, and nozzle size on piezoelectrically driven inkjet droplets," *Microfluidics Nanofluidics*, vol. 8, no. 5, pp. 575–586, 2010.
[26] C.-H. Wu and W.-S. Hwang, "The effect of the echo-time of a bipolar pulse waveform on molten metallic droplet formation by squeeze mode piezoelectric inkjet printing," *Microelectron. Rel.*, vol. 55, pp. 630–636, Feb./Mar. 2015.
[27] S. Desai and M. Lovell, "Modeling fluid–structure interaction in a direct write manufacturing process," *J. Mater. Process. Technol.*, vol. 212, pp. 2031–2040, Oct. 2012.
[28] B.-H. Kim, H.-S. Lee, S.-W. Kim, P. Kang, and Y.-S. Park, "Hydrodynamic responses of a piezoelectric driven MEMS inkjet print-head," *Sens. Actuators A, Phys.*, vol. 210, pp. 131–140, Apr. 2014.
[29] Ansys Corporation, "Introduction to acoustics," ACT_Acoustics_Extension_R145_v8, ed., 2013.
[30] O. Corporation. *Tables of Acoustic Properties of Materials*. Accessed: Jul. 30, 2018. [Online]. Available: http://www.ondacorp.com/tecref_acoustictable.shtml

KAI LI was born in Shandong, China, in 1988. He received the B.E. degree from the School of Mechanical Engineering, Shandong University of Technology, in 2012, and the M.E. and Ph.D. degrees in mechatronics engineering from the School of Mechatronics Engineering, Harbin Institute of Technology, China, in 2014 and 2018, respectively. He is currently a Lecturer with the Harbin Institute of Technology. His research interests include piezoelectric micro-jet and microfluidics.

JUNKAO LIU was born in Hebei, China, in 1973. He received the B.E. degree in mechanical engineering and the Ph.D. degree in mechatronics engineering from the School of Mechatronics Engineering, Harbin Institute of Technology, China, in 1995 and 2001, respectively. Since 2011, he has been a Professor with the School of Mechatronics Engineering, Harbin Institute of Technology. His research interests include ultrasonic driving, biomimetic robots, and simulations of parallel mechanisms with multi-degree of freedom.

HENGYU LI was born in Hebei, China, in 1973. He received the B.E. degree in mechanical engineering and the Ph.D. degree in mechatronics engineering from the School of Mechatronics Engineering, Harbin Institute of Technology, China, in 1995 and 2001, respectively. Since 2011, he has been a Professor with the School of Mechatronics Engineering, Harbin Institute of Technology. His research interests include ultrasonic driving, biomimetic robots, and simulations of parallel mechanisms with multi-degree of freedom.

NAIMING QI was born in Heilongjiang, China, in 1962. He received the B.E. degree in hydraulic technology, the M.E. degree in fluid transmission and control, and the Ph.D. degrees in precision instrument and mechanical engineering from the Harbin Institute of Technology, China, in 1984, 1990, and 2001, respectively. He joined the School of Astronautics, Harbin Institute of Technology, in 1990, where he has been a Professor since 2002. He is currently the Leader of the Aircraft Electromechanical Integration Research Group and a member of the China Space Society, the National Gas Lubrication Specialized Committee, and the American Institute of Aeronautics and Astronautics. His research interests include automatic docking and testing technology of aircraft electromechanical integration, space control and intelligent docking technology, UAV motion planning and advanced recovery technology, dynamics and distributed control technology of super-large aircraft, multi-dimensional micro-low gravity simulation of spacecraft, and space equipment development technology.

WEISHAN CHEN was born in Hebei, China, in 1965. He received the B.E. and M.E. degrees in precision instrumentation engineering and the Ph.D. degree in mechatronics engineering from the Harbin Institute of Technology, China, in 1986, 1989, and 1997, respectively. Since 1999, he has been a Professor with the School of Mechatronics Engineering, Harbin Institute of Technology. His research interests include ultrasonic driving, smart materials and structures, and bio-robotics.